Flame-particle interaction inside a packed bed of cooled particles

Mohammadhassan Khodsiani, Frank Beyrau, Benoît Fond

Flame-particle interaction inside a packed bed of cooled particles

M. Khodsiani[1], F. Beyrau[1], and B. Fond*[2]

[1]Chair of Technical Thermodynamics, Universitätsplatz 2, 39106 Magdeburg, Germany
[2]ONERA, the French Aerospace Lab, Department of Aerodynamics, Aeroelasticity and Aeroacoustics (DAAA), Paris-Saclay University, 92190 Meudon, France

Abstract

The aim of this work is to investigate the interaction between a premixed methane-air flame and particles within a packed bed. The opacity of the conventional packed bed reactors hinders the implementation of the optical diagnostics, so that no spatially resolved experimental data are available for numerical simulations. In this work, a two-dimensional cylindrical packed bed design is designed to allow for a direct line-of-sight which allow optical measurements with high spatial resolution. To replicate reactor start-up conditions, internally cooled aluminum cylindrical particles are used, and cylinder-specific heat transfer rates are measured. Telecentric chemiluminescence imaging is performed to observe the two-dimensional flame front position and geometry relative to the surrounding cylinders. Flames stabilize at different positions based on inflow velocity and equivalence ratio, and a correlation is established between flame tip to cylinder stand-off distance and the flame to cylinder heat transfer rate, when normalized to the theoretical flame thermal power. This study provides resolved flame front position and heat transfer rates for a well-defined geometry with intense flame-particles interactions, serving as validation data for numerical simulations.

Introduction

Many chemical processes are designed to transform material in the form of large particles (larger than a few millimeters in size) that travel at a slow pace through a reactor. These reactors are known as packed bed reactors and they are used for particle transformation process such heating, drying, pyrolysis, calcination, and gasification. Those reactors significantly contribute to large CO_2 emission of process industries.

The temperature distribution within the bulk solid, as well as the gas composition surrounding it, are directly determined by the extent and location of the flame within the void space between the particles [1]. Both parameters play a crucial role in the heat and mass transfer between the bulk and the flame, which ultimately impacts the quality of the final product and the energy efficiency of the process.

Flame-wall interactions (FWI) in combustion engines and porous inert media (PIM) combustion are typically two separately treated area of combustion, but combustion in packed bed reactors directly relate to both of them. In nearly all configurations with a flame, walls play a major role in flame propagation by means of radical exchange, heat exchange and also by inducing a boundary layer. This is a two-may coupling, as the wall affects the propagation of the flame by means of inducing a boundary layer, exchanging radicals and dissipating heat, and the flame in return heats the particle up. The specific wall area per unit volume dictates the strength of this coupling.

In case of low specific area per volume, as in the internal combustion engines and gas turbines, thorough experimental and numerical investigation have addressed various aspects of the flame-wall interaction (FWI). [2, 3].

On the other hand, combustion in porous inert media (PIM), which has gained attention as a new low NO_x[4, 5], lies on the "high coupling" side of the interaction as there is a high specific area of particle surface per volume. There the fuel-air mixture combusts in the interstices and pores of a porous inert media such as ceramic foams, pellets or packed beds.

In the context of the interaction of a flame and solid surfaces, a Peclet number is defined as the ratio of the distance from the wall at which the flame quenches (δ_Q), to the Zeldovich premixed laminar flame thickness (δ_F), that is, Pe=δ_Q/δ_F. For porous media burner it is the ratio of the pore size to the laminar thickness. A minimum Pe for the flame to propagate inside a porous medium is reported to be 65 [4]. Considering a regular spherical packed bed of particles and a methane air mixture, this translates into a minimum sphere diameter of 10 mm diameter with a pore size of 2.5 mm for the sphere to propagate inside the packing. A few experimental studies describe the propagation of the bulk flame zone in the interstices of the packed bed placed in a quartz glass tube [6, 7]. Nevertheless, the harsh scattering of light inside the packed bed and 3D-flame front were among the obstacles to an accurate and highly-resolved detection of the flame front.

In short, there is a need for an accurate description of the systems in which a reactive gas flows through a packing of particles. Also, CFD simulations must be validated as the high volume specific surface ratio means that the thermodiffusivity and wall chemistry play an important role. Obtaining unambiguous data in a

*Corresponding author: benoit.fond@onera.fr

setup with well defined boundary conditions is central to the validation of numerical simulations . Existing set of of experimental data do not allow such validation, as a) their flame image recordings incorporate complex 3D-effects b) the temperature of the particles is now known c) the geometry of the bed can not be fully reconstructed in simulations.

In this work we elaborate on the design of a cylindrical packed bed assembly in which a 2D flame can be stabilized between the cylinders. The cylindrical geometry also allows for a line-of-sight optical access. The first version of this assembly includes cooled cylinders to accurately compare with simulations and to replicate cold start-up conditions. Wall chemistry is expected to have less impact on flame propagation under these conditions than uncooled particles, which will be implemented in the next phase of the work. Prior to the flame studies, the uniformity of the temperature along the cylinder and the inflow velocity are verified to ensure two-dimensionality of the flow field and thermal boundary conditions. The impact of flame position and extent on flame to particle heat transfer is studied using telecentric imaging of the reaction and a double calorimetric technique. The experiments are performed under different equivalence ratio and inflow velocity conditions.

Two dimensional flame in a packed bed setup

In the design of the two-dimensional packed bed burner, three criteria are taken into account, a) transferabiliy and reproducibility of the experimental results, b) relevance of both geometry and boundary conditions to the packed beds in the industry and their flow specifications, c) allowing for measurements of quantities such as wall temperature, gas velocity, temperature and also species concentration.

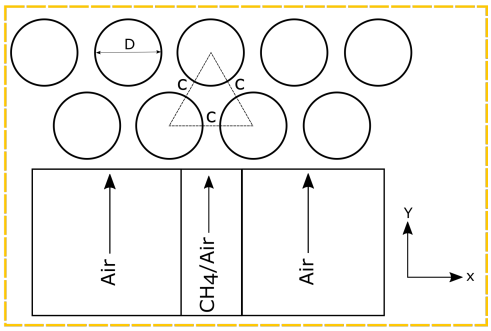

Figure 1: a) A cross-section of the packed bed assembly in the central region. Here the cylinder-to-cylinder distance (c) is 1.23 diameter D, resulting in a porosity of 40% packed bed porosity.

The geometry of the experimental setup comprises a slit burner and a packed bed of cylindrical particles. A cross sectional view of the cylinder arrangement in the central region is given in Fig. 1. As shown, rows of cylinders are offsetted by half the center to center distance c, imposing turns to the flow similar to spherical packed beds. The slit burner is designed to supply a uniform two-dimensional flow all along the cylinder length axis. It is composed of an inner duct delivering fuel/air mixture and an outer duct shielding the mixture by a co-flow of air. The mixture of fuel and air flows between the two cylinders in the center of the first row.

To set the porosity, taken as void fraction here, the distance c can be adjusted. Eq. (1) is used to calculate the porosity within a unit cell defined as the dashed triangle which connects the particle centers in Fig. 1.

$$1 - \frac{\pi}{2\sqrt{3}}\left(\frac{D}{c}\right)^2 \tag{1}$$

As described in the introduction, flame-particle interaction is largely affected by the porosity. To have a porosity of 40%, relevant to the typical spherical packed beds, the distance c was chosen to be 1.23 D. Thus, the reactive flow inside the cylindrical packed bed is exposed to a similar level of porosity and tortuosity. The specific area of the solid/gas boundary is only 33% lower than a spherical packed bed. The cylinder diameter D is 10 mm, leading to a minimum gap of 2.3 mm between the particles, corresponding to the limit Peclet number of porous media burner and and therefore is the case of intense interaction between the flame and the particles.

The main advantage of this geometry is its through optical access which enables the implementation of line-of-sight optical diagnostics. The two-dimensionality of the flow and of the gas thermochemical state remains a significant consideration for the following reasons: 1) It simplified the flame behaviour description in both experiments and numerical simulations. 2) It avoids the signal averaging error induced when implementing diagnostics such as chemiluminescence imaging and schlieren, reliant on the integration of light all along the line-of-sight.

A three dimensional view of the assembly of the packed bed assembly and burner is shown in Fig. 2a

To keep the flow two-dimensional, end walls are placed in the cylinder axes normal direction to confine the flow between the cylinders and avoid the apparition of a third flow velocity component which would be otherwise be caused by the escape of the flow through the open ends of the cylinders. For this reason, the uncooled cylinders are also extended past the holding frames to maintain similar pressure drop in the end region than through the cylinder array. A pair of optical windows on front and back side of the packed bed is used to keep the optical access. Also, side walls are also used to position the aluminum holding plates and to confine the co-flow and central jet and facilitate comparison with numerical simulations. The cylinder holder plates were machined as to provide an extended optical access to a large connected region, shown in Fig. 2b. This optical access covees the inflow region between the duct exit region below the first row, the region of the reactive flow between the three cooled cylinders, and also a large region of burnt gases. The two dimensionality of the inflow conditions was verified by particle image velocimetry measurements, described in [8]. The inflow

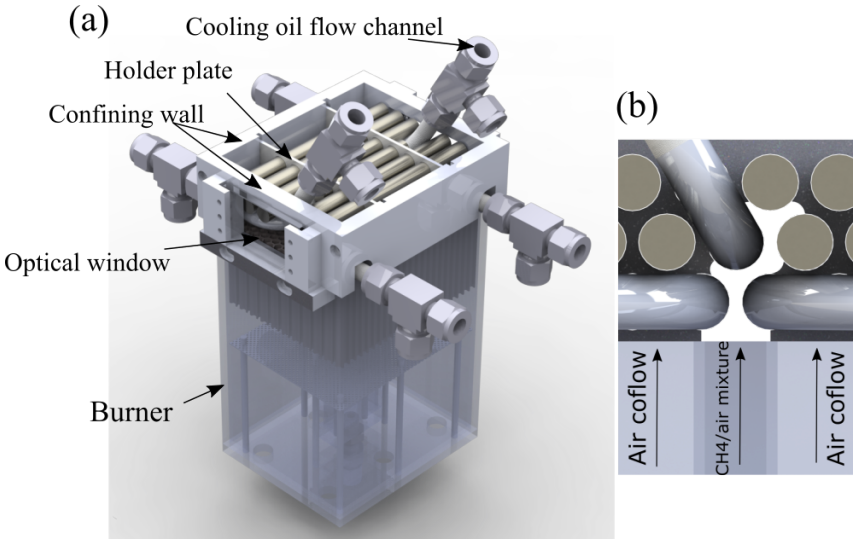

Figure 2: a) Finally manufactured assembly of the cylindrical packed bed and burner b) front view of the assembly; white area delineates the region with optical access)

velocity variation along the cylinder axis was found to vary by less than 5%.

Flame front imaging

A telecentric imaging system was employed to both detect the two dimensional flame reaction zone position, and to measure the real geometry of the rig compared to ideally conceived geometry. Chemiluminescence emission from the intermediate radicals is used to mark the position and shape of the flame front through the line-of-sight optical access in between the cooled cylindrical particles. CH* chemiluminescnece at 431 nm and C_2* at 471 nm are recorded to mark the reaction zone. The error in the marked flame front using visible emission should be limited to around a few percent of the laminar flame thickness [9]. That the maximum intensity position of C_2* and CH* emission are pretty similar is also experimentally demonstrated in [10]. Otherwise integration of the emitted light from the two radicals would have led to the detection of an artificially thicker flame front. However, imaging by conventional lenses would cause perspective distortion along the line-of-sight, so that the flame zone closer to the lens would be imaged with a larger magnification compared to the regions further from the lens. This finally leads to a loss of resolution when collecting all emitted light along the line of sight. To remedy this problem, a telecentric lens (Edmund Optics #62-912) was employed to maintain the same magnification all along the line of sight over which the chemiluminescence is emitted, as illustrated in Fig. 3(a). The telecentric lens axis is aligned with the cylinders axes and mounted on a sCMOS camera (PCO Edge 5.5) to record the chemiluminescence emanating from the reaction front over an exposure of 100 ms. The telecentric lense was equiped with a 500 nm short pass filter (Edmund Optics #84-719) to distinct the blue chemiluminescence from stray light and thermal radiation.

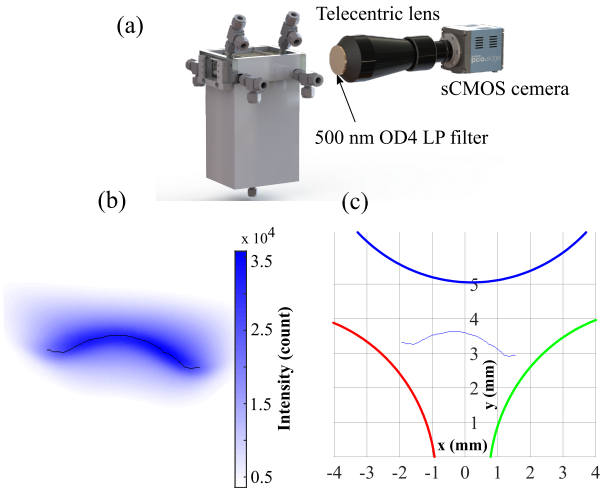

Figure 3: a) Telecentric lens mounted on the sCMOS camera and aligned with through optical access; b) Recorded methane-air flame image and superimposed extracted skeleton

Image processing

An image processing algorithm is developed in MATLAB to accurately detect the cylinder boundaries as well as the location of the two dimensional flame front. This is both to assess the real geometry of the bed, and to reveal the location of the reaction front with respect to this geometry. A gradient-based algorithm detects the points lying on the edges of the top, right and left cylinders. Fitting a circle to those points, the center coordinates of cylinders is found. Blue, green and red circles of Fig. 3(c) are the fitted circles and delineate the detected edges of the top, right and bottom cylinders, respectively. Images of the flame luminos-

ity are then recorded as shown in Fig. 3(b). Nevertheless, the accurate detection of the reaction front requires the extraction of the high intensity core of the flame in Fig. 3(b). In doing so, an algorithm is developed to access the centreline of the reaction zone by a combination of a Canny edge detection algorithm [11], to isolate the reaction zone, and then a subsequent skeletonization to extract the high intensity core of that the reaction zone. The extracted centerline, being a one pixel thick line is superimposed on the blue reaction front in Fig. 3(b). In order to mark the location of the methane-air flame relative the cylinders, the detected cylinder walls and the extracted flame centerline are put together on a grid in Fig. 3 (c). This forms the premise for the discussion of flame front location under different operating conditions in section .

Internal cylinder cooling and heat transfer measurements

Besides the velocity uniformity, the temperature of the aluminum cylinders must be kept uniform along the cylinder length to make sure that flame stabilizes at the same height and lateral position all along the cylinder length, forming a two dimensional flame surface. Therefore, a sufficiently high flow of coolant must flow inside the hollow aluminum cylinders to prevent an oil temperature increase along the cylinder direction. Two cooling circuits are designed to feed a high flow of silicon oil into the cylinders cooling channels. Based on the flame power, oil coolers were selected to provide a high enough oil flow rate to reduce the cylinders temperature down to about 100 °C while minimizing the surface temperature variations along the cylinder axis to below 1°C. Surface temperature measurements are described in [8].

Heat transfer rates from the flame to to each individual cylinder are important quantities in the investigation of the interaction between the flame and the particles. To measure the heat transfer to each cylinder, we resort to a double calorimetric technique. First, through Eq. 2, the heat transfer rate is related to the oil temperature increase and its mass flow rate as it flows through the cylinder. T_i and T_o are the oil temperature measured at the inlet and outlet of the top cylinder. The same equation holds for the side cylinders.

$$\dot{Q}_{\text{Top cylinder}} = \dot{m}_{\text{oil}} c_{p_{\text{oil}}} (T_o - T_i) \tag{2}$$

To measure the oil temperature rise in the presence of the flame, Resistance Temperature Detection (RTD) sensors with a diameter of 1 mm were inserted to the inlet and outlet of the cylinder. Probes are four-wired platinum resistance thermometers with class A accuracy, corresponding to a ±0.15 °C absolute temperature accuracy and an excellent capability to measure relative temperature variations due to very low drift. Such temperature resolution was required as a high silicon oil flow rate is used to keep the oil temperature rise below one degree, ensuring the uniformity of the temperature uniformity all along the cylinder. A second calorimetric technique was used to measure the oil mass flow rate. This technique relates the oil mass flow rate to another temperature difference. These in-house designed calorimetric flowmeters were implemented in the cooling circuit. More details on the method can be found in Ref. [8]

Having measured the oil mass flow rate and the inlet to outlet oil temperature rise, Eq. 2 yields the heat transfer to the cylinder which is discussed in conjunction with the flame chemiluminescence imaging measurements later in section .

Results

In this section, two parameters, namely, the inflow velocity (u) and the equivalence ratio (ϕ) are altered, and the flame position and geometry is discussed together with the heat transfer to the cylinders.

Chemiluminescence images recorded between the cylinders under three different operating conditions are shown in Figure. 4(a,b,c). Blue region in between them delineates the methane-air reaction front, while black areas mark the cylinders. The extracted flame skeletons are shown in Fig. 4(d) to better discern the flame position and geometry under three different conditions. A stable flame is recorded as shown in Fig. 4 at the reference condition, an inflow velocity of 0.3 m/s and stoichiometric condition. A high chemiluminescence intensity region, with a thickness of about 600 μm, marks the location of the reaction zone in between the cylinders. The extracted flame skeleton of Fig. 4(d) mark the exact geometry and extent of the flame front. The uppermost flame skeleton point is located at a distance of around 3 mm from the top cylinder, and the flame skeleton horizontally extends over a length of about 3.5 mm. A high pressure region, due to the stagnation of the fast burnt gases downstream of the flame front, is induces near the top cylinder. This stagnation region pushes the flame front further upstream. The flame front has a negative curvature, flattening on the side, which may be caused by the presence of a low velocity recirculation zone combined with the slower flame speed due to flame to wall heat losses.

Maintaining ϕ at 1 and slowing u down to 0.25 m/s, the flame front contracts and moves upstream considerably to the location observed in Fig. 4(b); as also observed in the extracted skeleton in Fig. 4(d). With the equivalence ratio and the laminar flame speed remaining untouched, the flame front descends by one cm upstream to a region where the gas speed under the current inflow velocity (u=0.25 m/s) is as fast as it was for inflow velocity (u) of 0.3 m/s. In addition, compared to the reference condition, the flame front is considerably flatter and the curvature is even slightly positive. This positive curvature is probably due to the thinner boundary layer and the smaller size of the recirculation region, which leads to a top hat reactant velocity profile. In this case, the positive flame curvature near the wall might have been induced by the slowed flame speed due to the heat losses when approaching the walls.

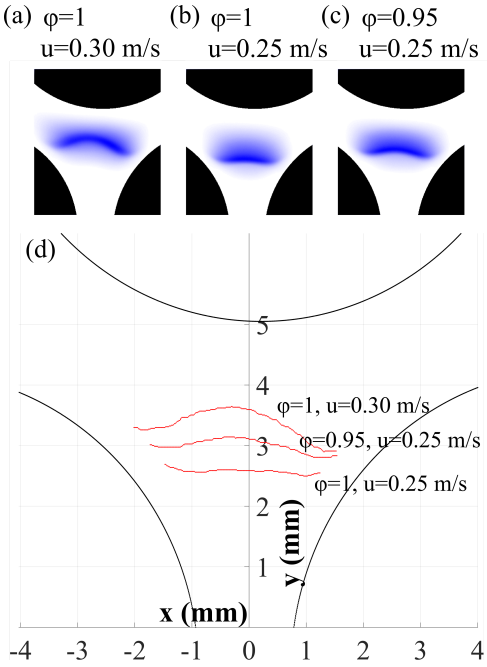

Figure 4: a to c) CH* chemiluminescence recorded under different operating conditions; d) detected flame skeletons. Black lines on the top, left and right are the detected edge of the particles

Transiting to the last operating condition, u is matintained at 0.25 m/s while ϕ is decreased to 0.95. A lean mixture slows the laminar flame speed down, and therefore the reaction front ascends half a centimeter downstream to settle in a region of lower gas velocity. As shown in Fig. 4c and also the flame skeleton of Fig. 4d, the reaction front expands, its curvature becomes more pronounced compared to the stoichiometric condition, but remains still a lower than the the curvature of the flame at the reference condition.

The rate of flame to particle heat transfer is measured for the top and bottom cylinders three operating conditions. In order to take the variation of the total flame power into account, when comparing the heat transfer rates under different operating conditions, a parameter named heat transfer efficiency (η) is introduced. η is defined as the ratio of the heat transferred to the cylinder divided by the theoretically calculated flame power, being the product of the flow rate of the fuel and its lower heating value.

Having detected the flame skeletons and measured the flame to particle heat transfer rate, the influence of the flame stabilization position on the heat transfer to the cylindrical particles can be quantified. To do so, the distance between the tip of the flame skeleton to the cylinder surface is evaluated for both top and bottom cylinders and plotted against the heat transfer efficiency (η) in Fig. 5. The heat transfer efficiency of both top and bottom cylinder diminishes as the flame front moves away from the cylinder. For the top cylinder, this might be attributed to a lower temperature gradients over the cylinder surface as the flame front moves further upstream away from the cylinder. In case of the bottom cylinders, the flame front moves downstream away from the cylinders, exposing a lower portion of the cylinder surface to the hot and fast burnt gas. This in turn leads to a weaker heat transfer.

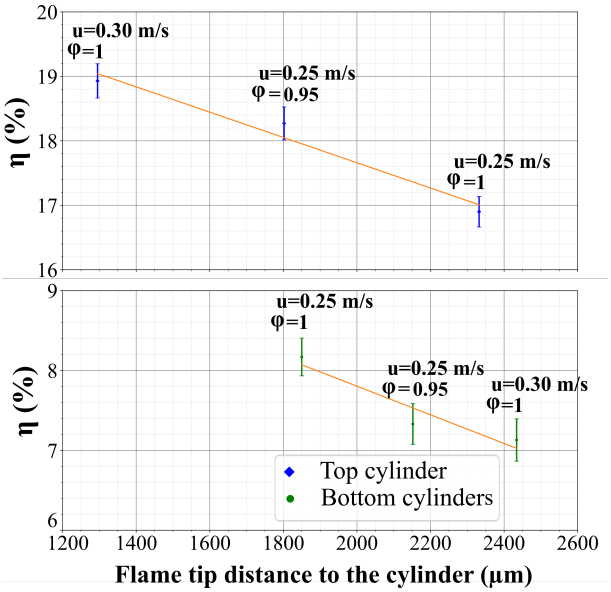

Figure 5: Variation of the heat transfer efficiency (η) with the stand-off distance of the flame skeleton tip from the top and bottom cylinders. The corresponding operating condition of each data point is annotated.

Conclusion

Spatially-resolved experimental data on the flame-particle interaction in a packed bed model reactor are essential to develop and validate numerical models. Therefore a two-dimensional packed bed of cooled cylinders was conceived and operated. Telecentric imaging of the CH* chemiluminescence emanating from the reaction zone, in conjunction with flame-to-particle heat transfer measurements, revealed the effect of the flame extent and position on the individual flame-to-particle heat transfer. A flame was stabilised above the reactant inflow in the void space between the first and second row of cylinder at a Reynolds number of 250. Due to the closeness of the flame to the cylinders, a significant flame to wall heat transfer was measured, being 25 % $\pm$ 2.5% of the total flame thermal power. By varying the inflow velocity and equivalence ratio, the reaction front was stablized at different locations downstream of the narrow gap between the cylinders in the bottom row. These changes also led to different heat transfer distribution between the upstream and downstream cylinders. Also, a correlation was found between the flame tip to cylinder stand-off distance and the heat transfer rate efficiency to that cylinder. These data provide the heat transfer rate, thermal boundary condition and reaction front stabilization position over a fully characterised geometry precluding any spatial ambiguity. They can therefore be directly exploited to validate

the implementation of wall heat transfer and chemistry models in direct numerical simulations. In future works, flow velocity measurements by laser Doppler anemometry will allow to interpret the flame position and shape with respect to complex geometry of the flow and to determine the local flame consumption speed. Moreover, we will also investigate the case of hot cylinder temperature, replacing the three cooled cylinders by ceramic cylinders.

Acknowledgment

The authors gratefully acknowledge funding by the Deutsche Forschungsgemeinschaft (DFG, German Research Foundation) – Project-ID 422037413 – TRR 287.

References

[1] B. Krause, B. Liedmann, J. Wiese, S. Wirtz, and V. Scherer, Coupled three dimensional DEM-CFD simulation of a lime shaft kiln-Calcination, particle movement and gas phase flow field, *Chemical Engineering Science* **134**, 834 (2015), ISSN 00092509.

[2] T. J. Poinsot, D. C. Haworth, and G. Bruneaux, Direct simulation and modeling of flame-wall interaction for premixed turbulent combustion, *Combustion and Flame* **95**, 118 (1993), ISSN 00102180.

[3] C. Jainski, M. Rißmann, B. Böhm, J. Janicka, and A. Dreizler, Sidewall quenching of atmospheric laminar premixed flames studied by laser-based diagnostics, *Combustion and Flame* **183**, 271 (2017), ISSN 15562921.

[4] D. Trimis and F. Durst, Combustion in a Porous Medium-Advances and Applications, *Combustion Science and Technology* **121**, 153 (1996), ISSN 0010-2202.

[5] S. Wood and A. T. Harris, Porous burners for lean-burn applications, *Progress in Energy and Combustion Science* **34**, 667 (2008), ISSN 03601285.

[6] M. Okuyama, T. Suzuki, Y. Ogami, M. Kumagami, and H. Kobayashi, Turbulent combustion characteristics of premixed gases in a packed pebble bed at high pressure, *Proceedings of the Combustion Institute* **33**, 1639 (2011), ISSN 15407489.

[7] D. Wu, H. Liu, M. Xie, H. Liu, and W. Sun, Experimental investigation on low velocity filtration combustion in porous packed bed using gaseous and liquid fuels, *Experimental Thermal and Fluid Science* **36**, 169 (2012), ISSN 08941777.

[8] M. Khodsiani, R. Namdar, F. Varnik, F. Beyrau, and B. Fond, Spatially resolved experimental investigation of particle-flame interaction in a two-dimensional model packed bed, *in revisions in Particuology* (2023).

[9] M. Bellenoue, T. Kageyama, S. A. Labuda, and J. Sotton, Direct measuremrment of laminar flame quenching distance in a closed vessel, *Experimental Thermal and Fluid Science* **27**, 323 (2003), ISSN 08941777.

[10] J. Kojima, Y. Ikeda, and T. Nakajima, Spatially resolved measurement of OH, CH, and C2 chemiluminescence in the reaction zone of laminar methane/air premixed flames, *Proceedings of the Combustion Institute* **28**, 1757 (2000), ISSN 15407489.

[11] J. Canny, A Computational Approach to Edge Detection, *IEEE Transactions on Pattern Analysis and Machine Intelligence* **PAMI-8**, 679 (1986), ISSN 01628828.